



# **iJRASET**

International Journal For Research in  
Applied Science and Engineering Technology



---

# **INTERNATIONAL JOURNAL FOR RESEARCH**

IN APPLIED SCIENCE & ENGINEERING TECHNOLOGY

---

**Volume: 8      Issue: XI      Month of publication: November 2020**

**DOI: <https://doi.org/10.22214/ijraset.2020.32328>**

**[www.ijraset.com](http://www.ijraset.com)**

**Call:  08813907089**

**E-mail ID: [ijraset@gmail.com](mailto:ijraset@gmail.com)**

# Magnet-Simulink Co-Simulation of Eight-Pole Heteropolar Radial Hybrid Magnetic Bearing

Yijian Duan<sup>1</sup>, Zhixian Zhong<sup>2</sup>

<sup>1, 2</sup>College of Mechanical and Control Engineering, Guilin University of Technology, 541000 Guilin, China;

**Abstract:** Aiming at the control of eight-pole heteropolar radial hybrid magnetic bearing (HRHMB), The Magnet-Simulink co-simulation method is proposed. First, the program block diagram of PID control magnetic system is built in Simulink. Then the model of the eight-pole HRHMB in Magnet is imported into the control program of Simulink. Finally, the Magnet-Simulink co-simulation model of the eight-pole HRHMB system controlled by PID is established. The results of simulation show that the Magnet-Simulink co-simulation method can realize real-time monitoring of rotor displacement, current, electromagnetic force, magnetic flux density and other parameter changes. Therefore, the Magnet-Simulink co-simulation method not only improves the efficiency of magnetic bearing control simulation, but also provides a new idea for exploring the rationality of the structural parameter design and working principle of the magnetic bearing.

**Keywords:** Magnet, Simulink; co-simulation, eight-pole Heteropolar Radial Hybrid Magnetic Bearing (HRHMB), PID control.

## I. INTRODUCTION

Hybrid magnetic bearings (HMB) use the bias magnetic flux by the permanent magnet to replace the bias magnetic flux in the control coil. Because HMB has the advantages of low power consumption, small size, long life, etc. Therefore, it has broad application prospects in many industrial applications such as energy storage flywheels, wind power generation, turbomolecular pumps and compressors [1-3].

HMB can be roughly divided into two categories, namely homopolar hybrid magnetic bearing and heteropolar hybrid magnetic bearing [4-5]. Among them, the HRHMB has received wide attention from scholars due to its shorter axial length and less magnetic leakage [6]. In [7], the HMB is analyzed by the equivalent magnetic circuit (EMC). Then, the finite element software is used for simulation and calculation. The research results show that when the magnetomotive force inside the permanent magnet increases, the bearing capacity and stability of the bearing can be improved. At the same time, when the bias magnetic flux is greater than half of the saturation magnetic flux, the actual bearing capacity is the largest. In [8], a 3-DOF electromagnetic bearing with annular radial control coil is proposed. This structure reduces the copper loss of the electromagnetic bearing structure by using annular coil. And, the weak cross coupling effect of 3-DOF electromagnetic bearing is proved by 3-D FEM. In [9], a new type of radial HMB structure is designed. Then, it is concluded that there is no coupling in the magnetic circuit of this HMB. Finally, a stable static suspension experiment was carried out. The experimental results show that this kind of magnetic bearing can significantly reduce power loss. In [10], Based on the six-pole HRHMB, the principle of designing the bias magnetic field of the magnetic bearing according to the smallest bearing capacity in each direction is proposed. Then the suspension force of the magnetic bearing was simulated and analyzed. The simulation results show that the suspension force in the X and Y directions within a certain range has good linear characteristics. In the meanwhile, the linear range in the x direction is greater than the linear range in the Y direction. In [11], Based on the EMC method, the design method of the eight-pole HRHMB structure parameters is derived. The experimental results show that the HRHMB designed by this method has excellent suspension performance. In [12], a twelve -pole HRHMB is designed, its EMC model is derived, and a twelve -pole HRHMB prototype is made. The simulation and experimental results show that the new HRHMB produces a large suspension force. At the same time, the linearity of suspension force, current and displacement is high.

Many scholars have carried out in-depth research on the structural design and control of HRHMB[13-15]. But most of the researches are limited to the finite element simulation of the magnetic bearing system without controller control, or monitoring the data through physical control. Therefore, the experiment is difficult and costly. And it is impossible to observe the magnetic field changes of the magnetic bearing system in suspension. However, the co-simulation method realize real-time monitoring of rotor displacement, current, electromagnetic force, magnetic flux density, and other parameter changes [16-17]. Furthermore, the working principle of the designed magnetic bearing structure is accurately analyzed. And this method provides a reference for the study of the structure of the electromagnetic bearing and the design of the controller.

### II. STRUCTURE OF EIGHT-POLE HRHMB

As shown in Fig. 1, the eight-pole HRHMB consists of a radial stator, a radial control winding, a rotor, and a block-shaped permanent magnet. In HRHMB, a stator with a circular outer periphery and 8 magnetic poles is used. Among the 8 magnetic poles, 4 control magnetic poles and 4 magnetic poles embedded in block permanent magnets are staggered. Then, the magnetic poles form an alternating magnetic pole arrangement of NS poles. And, in order to reduce the influence of eddy current and hysteresis, both the stator and rotor are laminated with 0.3mm silicon steel sheets.

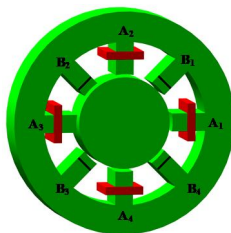


Fig. 1 Structure for the eight-pole HRHMB

### III. MAGNET-SIMULINK CO-SIMULATION

First, the eight-pole HRHMB structure model is established in the Magnet software. And, the model is imported into Simulink. Then, the PID controller is designed. Finally, the PID control block diagram of Magnet-Simulink co-simulation is built. As shown in Fig. 2, the input port is the coil current and load. And, the output port is voltage, displacement, speed and electromagnetic force. The gravity of the rotor in the vertical direction is 100N, and the load in the horizontal direction is 0N.

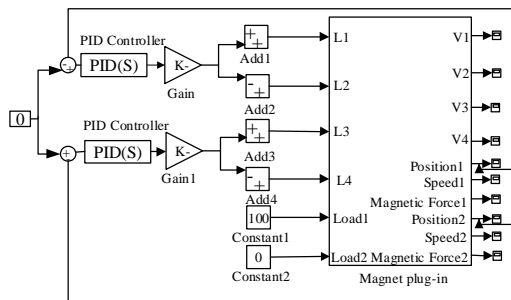
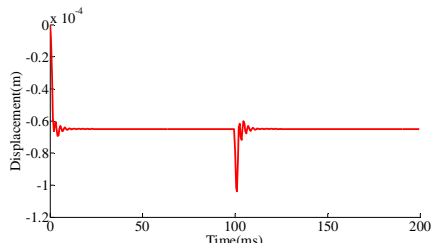


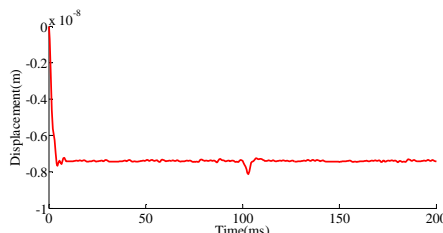
Fig. 2 PID Control Block diagram of eight-pole HRHMB System Magnet-Simulink Co-Simulation

#### A. Vertical Impact Simulation

As shown in Fig. 3 and Fig. 4, is that the rotor stably suspended in the equilibrium position is subjected to a vertical downward impact force of 100N. The rotor moves downward under the impact force. Then, the rotor reaches a maximum displacement of  $3.9 \times 10^{-5}$ m, as shown in Fig. 5 and Fig. 6. Since the air gap between the rotor and the magnetic poles of the stator is reduced, the air gap flux density of the magnetic poles B<sub>3</sub> and B<sub>4</sub> increased by 0.016T. As the air gap between the upper magnetic poles of the rotor and the stator is increases, the air gap magnetic flux density between the upper magnetic poles of the rotor and the stator is reduced by 0.045T. At this time, the PID controller increases the current of the coil of the magnetic pole A<sub>2</sub>. And, the magnetic flux density of the magnetic pole A<sub>2</sub> in the air gap increased by 0.28T. In addition, the PID controller reduces the current of the coil of magnetic pole A<sub>4</sub>, and the magnetic flux density of magnetic pole A<sub>4</sub> is correspondingly reduced by 0.39T. Due to the coupling effect, the maximum displacement of the rotor in the horizontal direction is  $8.12 \times 10^{-9}$ m. Therefore, the coupling between the vertical direction and the horizontal direction of the structure is small.

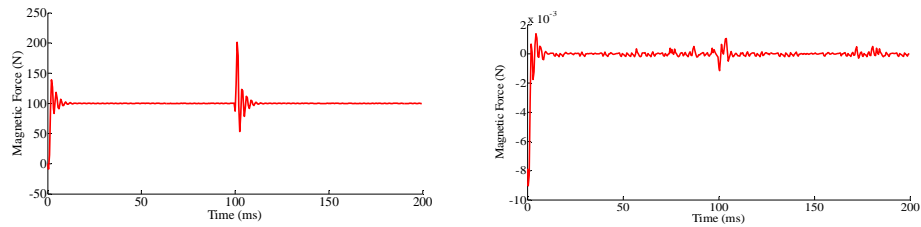


(a) The rotor's vertical displacement response



(b) The rotor's horizontal displacement response

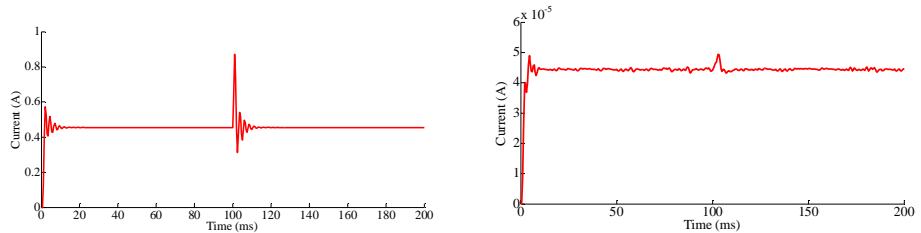
Fig. 3 The displacement response of the rotor under vertical impact



(a) The rotor's vertical electromagnetic force response

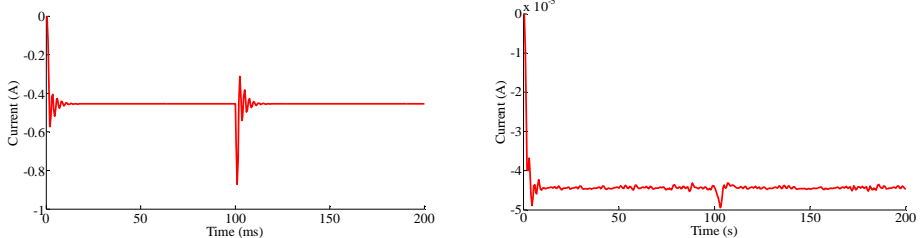
(b) The rotor's horizontal electromagnetic force response

Fig. 4 The electromagnetic force response of the rotor, under vertical impact



(a) The current response in the coil of A<sub>2</sub> pole

(b) The current response in the coil of A<sub>3</sub> pole



(c) The current response in the coil of A<sub>4</sub> pole

(d) The current response in the coil of A<sub>1</sub> pole

Fig. 5 The current response of the rotor under vertical impact

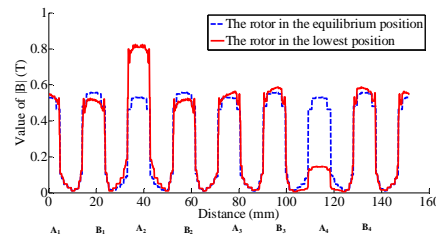


Fig. 6 The comparison of air gap flux density between the rotor in the lowest and equilibrium position

As shown in Fig. 3, is that the rotor moves upward under the action of electromagnetic force. Then it reaches the top position, as shown in Fig. 4, Fig. 5 and Fig. 7. The air gap between the lower magnetic poles of the rotor and the stator is increases. At the same time, the air gap between the upper magnetic poles of the rotor and stator is reduced. Then, the PID controller increases the current of the coil of magnetic pole A4. And the magnetic flux density of magnetic pole A4 has increased by 0.246T. The PID controller reduces the current of the coil of the magnetic pole A2, and the magnetic flux density of the magnetic pole A2 is reduced by 0.172T. Due to the need to balance the gravity of the rotor at all times, the magnetic flux density in the A2 magnetic pole air gap of the stator is larger than that of the A4 magnetic pole. In the end, the rotor is stably suspended in the equilibrium position.

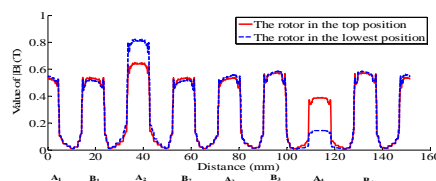
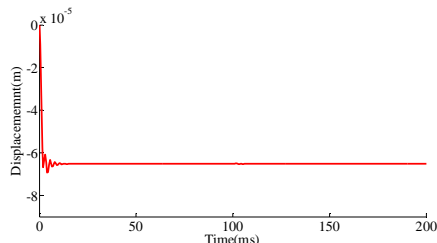


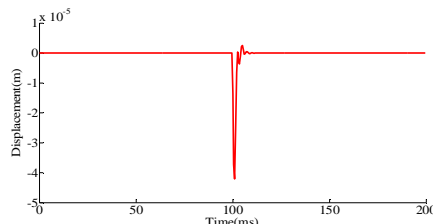
Fig. 7 The comparison of air gap flux density between the rotor in the lowest and top position

**B. Horizontal Impact Simulation**

As shown in Fig. 8 and Fig. 9. Because the rotor does not set an external load in the horizontal direction, the rotor quickly reaches a stable suspension state. Then, an impact force of 100N is applied to the rotor in the horizontal direction. At the same time, the rotor reaches a maximum displacement of  $4.21 \times 10^{-5}m$ . As shown in Fig. 10 and Fig. 11. When the air gap between the rotor and the left magnetic pole of the stator is reduced, the PID controller increases the current of the magnetic pole A1. Then, the magnetic flux density of the magnetic pole A1 in the air gap increases by 0.142T. In the meantime, the PID controller reduces the current of the magnetic pole A3, and the magnetic flux density of the magnetic pole A3 is reduced by 0.174T.

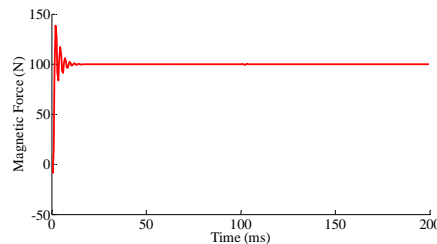


(a) The rotor's vertical displacement response

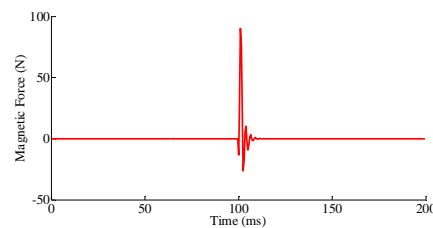


(b) The rotor's horizontal displacement response

Fig. 8 The displacement response of the rotor under horizontal impact

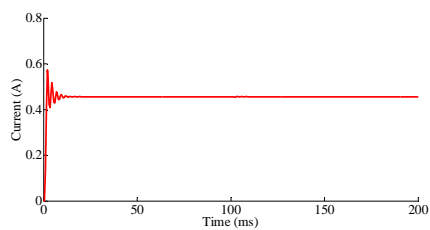


(a) The rotor's vertical electromagnetic force response

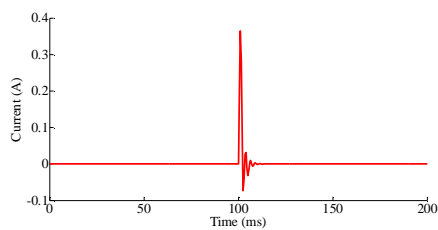


(b) The rotor's horizontal electromagnetic force response

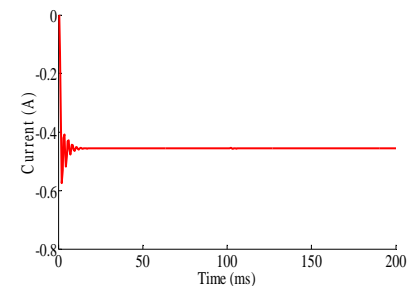
Fig. 9 The electromagnetic force response of the rotor under horizontal impact



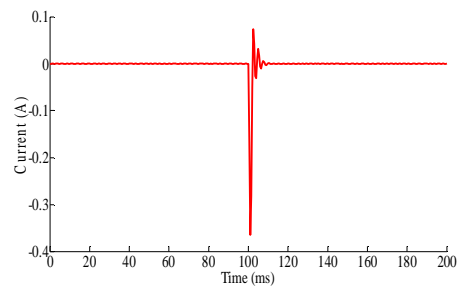
(a) The current response in the coil of A<sub>2</sub> pole



(b) The current response in the coil of A<sub>3</sub> pole



(c) The current response in the coil of A<sub>4</sub> pole



(d) The current response in the coil of A<sub>1</sub> pole

Fig. 10 The current response of the rotor under horizontal impact

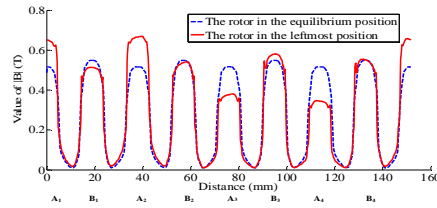


Fig. 11 The comparison of air gap flux density between the rotor in the leftmost and equilibrium position

As shown in Fig. 8, Fig. 10 and Fig. 12, is that the air gap between the rotor and the right magnetic pole of the stator is reduced, and the air gap between the rotor and the left magnetic pole of the stator is increased. At this time, the PID controller increases the current of the magnetic pole A3, and the magnetic flux density of magnetic pole A3 increases by 0.14T. The PID controller reduces the current of the magnetic pole A1, and the magnetic flux density of the magnetic pole A1 is reduced by 0.12T. Since there is no displacement in the vertical direction of the rotor, the magnetic flux density in the air gap of the magnetic poles A2 and A4 is basically unchanged. In the end, the rotor is stably suspended in the equilibrium position.

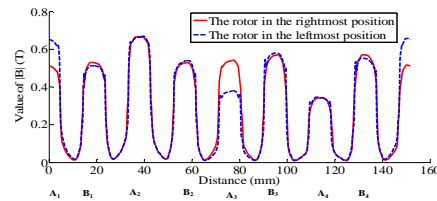
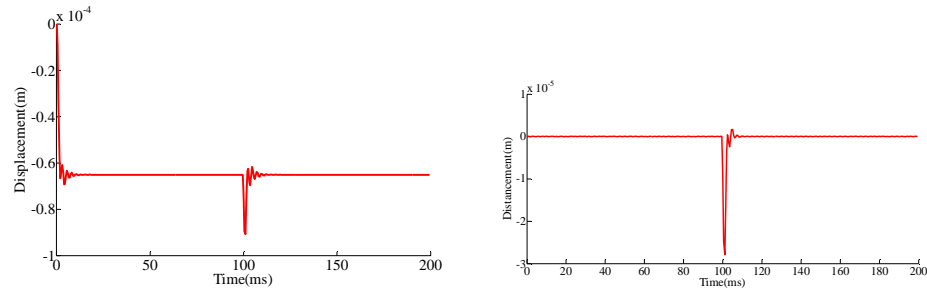


Fig. 12 The comparison of air gap flux density between the rotor in the leftmost and rightmost position

### C. Simulation Of Simultaneous Impact In Vertical And Horizontal Directions

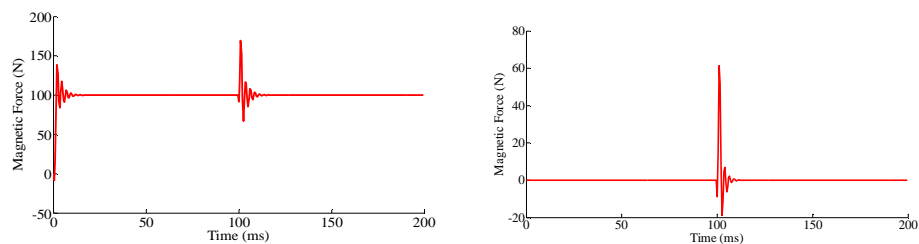
As shown in Fig. 13 and Fig. 14. When the stably suspended rotor receives an impact force of 100N in the vertical downward direction and horizontal leftward direction respectively, the rotor moves to the lower left under the impact force. As shown in Fig. 15 (a)-(d) and Fig. 16, is that the maximum displacement of the rotor in the horizontal and horizontal directions is  $2.79 \times 10^{-5}m$  and  $2.56 \times 10^{-5}m$ , respectively. At this time, the magnetic flux density of magnetic pole A2 and magnetic pole A1 increased by 0.158T and 0.112T, respectively. The magnetic flux density of magnetic pole A4 and magnetic pole A3 is reduced by 0.27T and 0.069T respectively.



(a) The rotor's vertical displacement response

(b) The rotor's horizontal displacement response

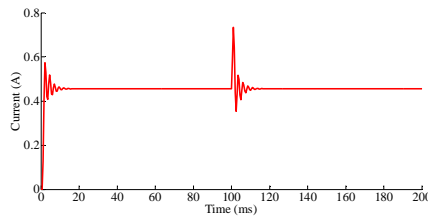
Fig. 13 The displacement response of the rotor under horizontal impact and vertical impact



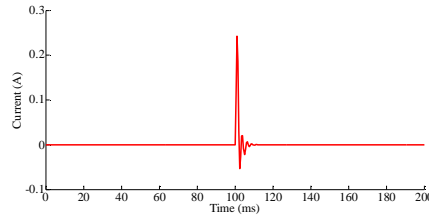
(a) The rotor's vertical electromagnetic force response

(b) The rotor's horizontal electromagnetic force response

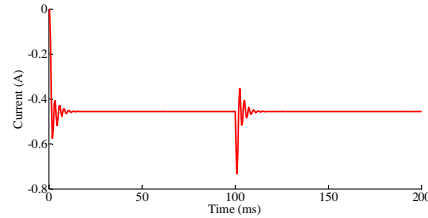
Fig. 14 The electromagnetic force response of the rotor under horizontal impact and vertical impact



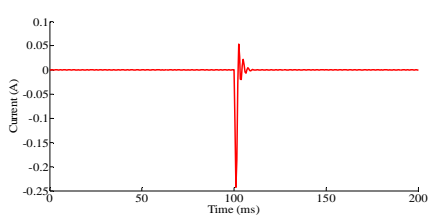
(a) The current response in the coil of  $A_2$  pole



(b) The current response in the coil of  $A_3$  pole



(c) The current response in the coil of  $A_4$  pole



(d) The current response in the coil of  $A_1$  pole

Fig. 15 The current response of the rotor under horizontal impact and vertical impact

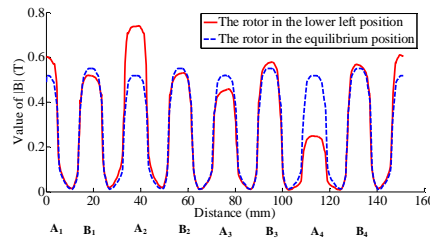


Fig. 16 The comparison of air gap flux density between the rotor in the lower and equilibrium position

As shown in Fig. 15 and Fig. 17, is that the magnetic flux density of magnetic pole A2 and magnetic pole A1 decreased by 0.118T and 0.108T, respectively. Then, the magnetic flux density of the magnetic pole A4 and the magnetic pole A3 increase by 0.146T and 0.084T correspondingly. Since the eight-pole HRHMB has a small coupling, the flux density of the other magnetic poles is almost unchanged. In the end, the rotor is stably suspended in the equilibrium position.

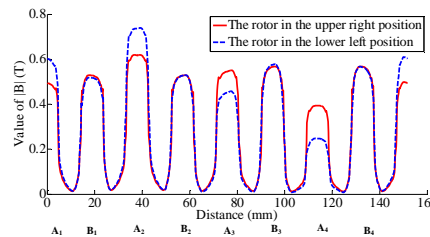


Fig. 17 Comparison of air gap flux density between the rotor in the lower position and the rotor in the upper right position

#### IV. CONCLUSIONS

In the paper, the program block diagram of PID control magnetic system is built in Simulink. Then the model of the eight-pole HRHMB in Magnet is imported into the control program of Simulink. Finally, the Magnet-Simulink co-simulation model of the eight-pole HRHMB system controlled by PID is established. The simulation results show that the Magnet-Simulink co-simulation method can realize real-time monitoring of rotor displacement, current, electromagnetic force, magnetic flux density, and other parameter changes. Therefore, the Magnet-Simulink co-simulation method not only improves the efficiency of magnetic bearing control simulation, but also provides a new idea for exploring the rationality of the structural parameter design and working principle of the magnetic bearing.

## V. ACKNOWLEDGMENT

This work was sponsored by the Guilin University of Technology scientific research fund (No.002401003438).

## REFERENCES

- [1] Mauro Andriollo, Roberto Benato, Andrea Tortella. Design and Modeling of an Integrated Flywheel Magnetic Suspension for Kinetic Energy Storage Systems. *Energies*, vol. 13, pp. 847, 2020.
- [2] K.X. Qian, P. Zeng, W.M. Ru, and H.Y. Yuan, New concepts and new design of permanent maglev rotary artificial heart blood pumps, *Medical Engineering & Physics*, vol. 28, pp. 383-388, 2006.
- [3] Bangcheng Han, Ziyuan Huang, and Yun Le, Design aspects of a large scale turbomolecular pump with active magnetic bearings, *Vacuum*, vol. 142, pp. 96-105, 2017.
- [4] Xu Yanliang, Dun Yueqin, Wang Xiuhue and Kong Yu, Analysis of hybrid magnetic bearing with a permanent magnet in the rotor by FEM, *IEEE Trans. Magn.*, vol. 42, pp. 1363-1366, 2006.
- [5] Andrew Kenny and Alan B. Palazzolo, Single Plane Radial, Magnetic Bearings Biased With Poles Containing Permanent Magnets, *Journal of Mechanical Design*, vol. 125, pp. 178-184, 2003.
- [6] Kenny A. Nonlinear electromagnetic effects on magnetic bearing performance and power loss, Ph.D. dissertation, Texas A&M University, College Station, Texas, 2001.
- [7] Huang Feng, Zhu Huangqiu, Xie Zhiyi, Parameter Design and Analysis for Two-degrees of Freedom Radial Hybrid Magnetic Bearings, *China Mechanical Engineering*, vol. 10, pp. 1143-1146, 2007.
- [8] Y. Zhong, L. Wu, X. Huang and Y. Fang, Modeling and Design of a 3-DOF Magnetic Bearing With Toroidal Radial Control Coils, *IEEE Trans. Magn.*, vol. 55, pp. 1-7, 2019.
- [9] Gao Sumei, Xu Longxiang, Study on Radial Permanent Magnet Biased Magnetic Bearing with Two degrees of Freedom, *Small & Special Electrical Machines*, vol. 11, pp. 11-14, 2007.
- [10] Ji Li, Xu Longxiang, and Jin Chaowu, Research on Six Magnetic Poles Heteropolar Radial Permanent Magnet Biased Magnetic Bearing, *China Mechanical Engineering*, vol. 24, pp. 730-735+741, 2013.
- [11] Zhao Xusheng, Deng Zhiqian and Wang Bo, Parameter Design and Realization of Permanent Magnet Biased Heteropolar Radial Magnetic Bearing, *Transactions of China Electrotechnical Society*, pp. 131-138+159, 2012.
- [12] Zhu Huangqiu, Shao Jiawei, A Novel Type of Heteropolar Radial Hybrid Magnetic Bearing Parameter Design and Performance Analysis, *Electric Machines & Control Application*, vol. 44, pp. 58-65, 2017.
- [13] T. Matsuzaki, M. Takemoto, S. Ogasawara, S. Ota, K. Oi and D. Matsuhashi, "Novel Structure of Three-Axis Active-Control-Type Magnetic Bearing for Reducing Rotor Iron Loss," *IEEE Transactions on Magnetics*, vol. 52, no. 7, pp. 1-4, July 2016.
- [14] K. Hijikata, S. Kobayashi, M. Takemoto, Y. Tanaka, A. Chiba, and T. Fukao, "Basic characteristics of an active thrust magnetic bearing with a cylindrical rotor core," *IEEE Trans. Magn.*, vol. 44, no. 11, pp. 4167-4170, Nov. 2008.
- [15] Mei Lei, Deng Zhiqian, Zhao Xusheng, et al. New configuration hybrid radial magnetic bearing[J]. *Transactions of China Electrotechnical Society*, vol. 24, pp. 13-18, 2009.
- [16] Duan Yijian, Zhong Zhixian, Cai Zhonghou, QI Yanying, Co-simulation of Magnet and Simulink for radial electromagnetic levitation system, *Journal of Guilin University of Technology*, 2020.





10.22214/IJRASET



45.98



IMPACT FACTOR:  
7.129



IMPACT FACTOR:  
7.429



# INTERNATIONAL JOURNAL FOR RESEARCH

IN APPLIED SCIENCE & ENGINEERING TECHNOLOGY

Call : 08813907089  (24\*7 Support on Whatsapp)